Control over phase separation and nucleation using a laser-tweezing potential

Finlay Walton, Klaas Wynne*
School of Chemistry, WestCHEM, University of Glasgow, UK

Control over the nucleation of new phases is highly desirable but elusive. Even though there is a long history of crystallisation engineering by varying physicochemical parameters, controlling which polymorph crystallises or whether a molecule crystallises or forms an amorphous precipitate is still a black art. Although there are now numerous examples of control using laser-induced nucleation, a physical understanding is absent and preventing progress. Here we show that the proximity of a liquid-liquid critical point or the corresponding binodal line can be used by a laser-tweezing potential to induce concentration gradients. A simple theoretical model shows that the stored electromagnetic energy of the laser beam produces a free-energy potential that forces phase separation or triggers the nucleation of a new phase. Experiments in a liquid mixture using a low-power laser diode confirm the effect. Phase separation and nucleation through a laser-tweezing potential explains the physics behind non-photochemical laser-induced nucleation and suggests new ways of manipulating matter.

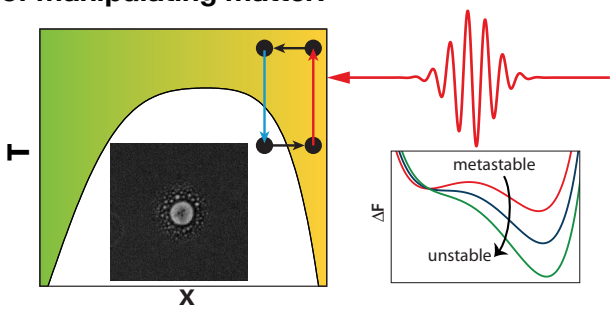

The nucleation of new phases such as crystals from solution is of enormous technological importance but poorly understood. Although the vast majority of pharmaceutical products and most fine and speciality chemical products are made in crystalline form, industrial crystallisation has changed little in the past 350 years and suffers from an embarrassing lack of control with sometimes unexpected and severe financial consequences.[1] Therefore, a deeper understanding of and control over (crystal) nucleation is of great importance.

Two decades ago, it was shown that nanosecond pulsed lasers can nucleate crystals in a supersaturated solution through a non-photochemical process.[2] Most significantly, it was shown that the crystal polymorph could be selected by the polarisation state of the laser.[3] Subsequent work has shown that laser pulses can induce nucleation of various crystals,[4,5] liquid crystals,[6,7] and bubbles.[8] It was initially suggested that the Kerr effect was responsible for laser-induced nucleation[2] but subsequent work has shown that the data are inconsistent with it.[9] Most disconcertingly, the reproducibility of polarisation-control over polymorph selection has been questioned while pulsed-laser induced nucleation appears to require impurity particles.[10] However, a laser-induced nucleation experiment using CW lasers did reliably show polarisation-control over polymorph selection.[11] Thus, it is fair to say that a physical understanding of these phenomena is still sorely lacking.

In a supersaturated solution, the crystal is the thermodynamically most stable state but is difficult to access in the absence of heterogeneous nucleation sites. In the simplest case, random fluctuations lead to the formation of a critical nucleus and ultimately a macroscopic crystal. As suggested by Frenkel for proteins[12] and more generally in non-classical nucleation theories,[13-15] the concentration fluctuations leading to nucleation may well be enhanced by the proximity of a liquid–liquid demixing critical point. However, recent molecular dynamics simulations of the kinetics of crystallisation found no special advantage of the proximity of the critical point on the nucleation rates.[16]

Here we show that concentration variations near the liquid-liquid binodal (phase-separation line) can be directed by use of a laser beam. Rather than using nucleation of a crystal from solution, we will use a mixture of two liquids and explicitly consider the nucleation of a phase-separated state. We will present a simple theoretical model that is able to predict the changes in the free-energy landscape caused by the laser as well as the dynamics of laser-induced phase separation. Experiments confirm these predictions and show that a relatively weak laser can induce phase separation in the neighbourhood of a liquid-liquid binodal. Time-resolved experiments demonstrate laser-induced nucleation of a new phase in the metastable region of the phase diagram.

These results have profound implications for the understanding of laser-induced nucleation phenomena and provide a new impetus for solving the recent controversial results. The large effect seen here near a liquid-liquid binodal could lead to new means of controlling matter using external forces.

Results and discussion

Theoretical model. The phase transition considered here occurs when two liquids are miscible at high temperature but separate into two phases when the temperature is lowered. The free energy of such a system can be described by the regular solution model (see supplementary section 1),[17] which is a simple but surprisingly comprehensive physical description of the mixing and demixing of two liquids. It uses the entropy of mixing of two species combined with a pairwise additive interaction between molecules. This theory then predicts the free energy of the system F as a function of the mole fraction of one of the liquids x_0.

The red curves in Figure 1(a) and (b) show the change in free energy when the mole fraction is changed in a small (0.1%) sub-volume in the sample. In the regime where the two liquids are fully mixed (Figure 1(a)), the free energy will always increase. However, in the metastable regime (at a temperature just below the binodal), after crossing a barrier, a new minimum in the free energy is reached corresponding to phase separation through homogeneous nucleation (Figure 1(b)).

When a laser beam is focussed into the small sub-volume, an additional enthalpy term $-n^2I$ (where n is the refractive index and I the laser intensity) must be added representing the total stored electromagnetic energy. This term lowers the free energy and constitutes a laser-tweezing trap[18] that will tend to pull in the liquid with the highest refractive index. This effect is universal and does not assume the presence of pre-nucleation clusters that could be laser trapped as physical objects.[19]

The blue and green curves in Figure 1(a) and (b) show the predicted effect of the additional laser-tweezing term. In the mixed regime, the laser has the effect of shifting the free energy minimum to higher mole fraction effectively laser-sucking the liquid with the higher refractive index out of the mixture. In the metastable regime, the laser lowers the barrier for phase separation and, at sufficient intensity, triggers the nucleation of a phase-separated droplet. Our calculations using the regular solution model with the additional stored electromagnetic energy term predict that these effects would occur at very reasonable laser powers of 10-100 mW (see supplementary section 1). Simulations using the Kramers diffusion equation including a laser-induced trap show that the high refractive-index liquid is sucked into the laser volume at a rate limited by diffusion (forming on a e^{-1} timescale of 0.5 seconds for a 2-μm radius spot size and the liquids used in the experiments) leaving behind a depleted volume (forming on a e^{-1} timescale of 1.7 seconds) that slowly fills up by diffusion from the rest of the sample (see Figure 1(c)).

Laser-induced phase separation (LIPS). Experiments were carried out on mixtures of nitrobenzene and decane, which behaves similarly to the well-known mixture nitrobenzene and hexane but is less prone to evaporation. The mixture has an upper consolute temperature in the bulk of $T_c = 295.96$ at critical mole fraction $x_c = 0.575$.[20] Samples ~12 μm thick were held in a cryogenically cooled stage (Figure 1(d)) mounted in a modified Olympus BX53 microscope, which allowed a 200-mW (maximum) 785-nm laser beam to be focussed in the sample.

Initial experiments were carried out at mole fractions and temperatures where the mixture is stable (above the binodal). We will refer to such experiments as laser-induced phase separation (LIPS).

When the laser is focussed in the sample while it is being observed by phase-contrast microscopy, a bright spot becomes visible (Figure 2(a)). This shows that LIPS takes place and that the fraction that is separated out of the mixture has a higher refractive index and must therefore be nitrobenzene rich. In supplementary section 2, we show that the refractive index change induced by LIPS is $\Delta n = 0.002$ corresponding to a change in mole fraction from critical to 0.589. The radial distribution (Figure 2(a)) shows a full width at half maximum (FWHM) of 4.5 μm and a depletion region minimum at a radius of 10 μm at steady state.

In order to confirm that the phase-separated region is nitrobenzene rich, the experiments were repeated in samples containing the dye methylene blue and fluorescence detection. The electron-withdrawing nitro group in nitrobenzene causes quenching of the fluorescence in proportion to the nitrobenzene concentration. As can be seen in Figure 2(b), using fluorescence detection, LIPS produces a dark spot surrounded by a brighter ring proving that the centre is indeed nitrobenzene rich and is surrounded by a nitrobenzene depleted region.

Temperature dependent experiments (see Figure 2(c)) show that the LIPS effect strongly increases in strength on cooling as the binodal is approached. This effect can be reproduced with the regular solution model with the laser tweezing term (not shown). The temperature dependence at mole fraction $x = 0.575$ (volume fraction $\varphi = 0.412$) can be fitted satisfactorily to a power law $(T-T_0)^{-1}$ where $T_0 = 23.3 \pm 0.1$°C, which is 0.3°C lower than the binodal temperature. As can be seen in Figure 2(d), the LIPS effect varies linearly with laser power between 30 mW (lasing threshold) and 90 mW and then saturates. The saturation is caused by the shade-off effect[21] inherent in phase-contrast microscopy that becomes significant when the LIPS spot becomes larger than a few micrometres. In addition to proximity to the binodal, the strength of the effect also depends on the nitrobenzene mole fraction. As can be seen in Figure 2(d), the strength of the LIPS effect follows an approximately bell-shaped curve as a function of

mole fraction peaking at the critical mole fraction. Time-dependent experiments show a mean e^{-1} formation time of 3.4 s and a decay time of 4.0 s.

Laser-induced nucleation. Laser-induced crystal-nucleation experiments in the past have been carried out on metastable (super-saturated) solutions.[2,3,9,22,23] In order to demonstrate that laser-induced nucleation can be caused by a laser-tweezing effect, we attempted to carry out experiments in the metastable region between the binodal and spinodal in the liquid-liquid phase-separation diagram. Unfortunately, because this metastable region is very narrow, such experiments proved very difficult due to the spontaneous nucleation of phase separation complicated by heating and Marangoni effects.[24]

However, laser-induced nucleation could be demonstrated when the temperature was set on the binodal temperature for a given nitrobenzene mole-fraction x. When the laser is switched on, a droplet is seen in phase-contrast imaging as in LIPS (see Figure 3(a)). Switching the laser off triggers the nucleation of a cloud of phase-separated droplets that ripens into a single large phase-separated droplet (Figure 3(b)-(d)). This droplet disappears again through remixing on a time scale of tens of minutes. The size of the nucleated droplet increases with both laser power and laser exposure time (see Figure 3(g),(h)). The effect was observed for $0.62 < x < 0.69$ (but not for mole fractions lower than critical) with the magnitude of the effect increasing as the critical point is approached (See Figure 3(e) and (f)).

When the laser is switched on, the LIPS effect draws nitrobenzene into the laser focus through diffusion, depleting the surrounding volume. If the nitrobenzene mole fraction of the sample is larger than critical and if the initial temperature is close to the binodal (see Supplementary Figure 5), it is to be expected that the enriched droplet remains in the mixed region while the depleted volume will fall below the binodal and becomes metastable. However, some of the laser power is absorbed, resulting in an estimated temperature rise of 0.5ºC (see supplementary section 4).[25] As the thermal diffusivity of nitrobenzene is three orders of magnitude greater than its diffusion coefficient, the heating effect will place both the enriched droplet and the depleted volume in the mixed region. When the laser is switched off, the temperature rapidly drops, placing the depleted volume below the binodal. It is this that triggers the nucleation of phase separated droplets in these experiments. For $x < x_c$, the depleted volume moves further into the mixed regime and nucleation does not occur.

Conclusions

Near phase-transition boundaries of any kind (liquid–gas, liquid–solid, liquid–liquid, *etc*.), concentration variations will take place that are likely to be greater near a critical point. We have shown here that a laser-tweezing potential, only relying on the stored electromagnetic energy in the laser focus, can direct such variations to enrich one component in a mixture or to trigger the nucleation of a phase-separated droplet by placing the mixture below the binodal line.

The effect described here is very different from laser-induced photothermal phase separation, which relies on liquid mixtures with a lower consolute boundary that is crossed through a trivial heating effect.[26-28] Earlier work on light-induced barodiffusion presented a similar theoretical model to the one used here but using the Navier-Stokes instead of the Kramers equations to describe laser-induced concentration variations.[29] The electrostrictive force introduced there is identical to the laser-tweezing potential discussed here but was disregarded in that work (under the assumption of infinitely short laser pulses) leaving only laser-induced photothermal phase separation. The LIPS effect is similar to but much larger than the optically biased diffusion of molecules described previously, which is only significant for molecules excited on resonance.[30]

The laser-tweezing potential induced phase separation near a liquid-liquid demixing critical point is likely to be related to previous observations of laser tweezing of amino acid crystals.[31] However, the latter experiments could only be carried out at an air-solution interface, implying a crucial role for evaporation and Marangoni effects.[24] The results presented here clearly require a repeat of those experiments in bulk samples and an exploration of non-trivial concentration effects caused by hidden liquid-liquid demixing critical points enhancing concentration variations.[12,14,32,33]

Since the laser-tweezing potential depth scales with the refractive index of the new phase and since nearly all solids have a higher refractive index than their corresponding liquid or solution phase, this effect can in principle explain all known laser-induced crystal-nucleation results, with the exception of nucleation induced by pulsed-laser induced vapour or plasma bubbles.

The effect described here does not depend on the presence of pre-nucleation clusters[14] that can be trapped or tweezed by the laser.[34] Instead, it creates a laser-tweezing potential well that lowers the free energy of the phase-separated state. This is a generic effect that does not only apply to poorly mixing liquids but to any mixture or solution. However, the ease with which the laser-tweezing potential can initiate phase separation is enhanced near a liquid-liquid demixing critical point or binodal line. Phase manipulation and nucleation can be induced with a straightforward low-power laser diode. This suggests that this effect can be used to control matter in a range of practical applications.

Methods

Materials

Experiments were carried out on nitrobenzene, decane, and methylene blue (Sigma Aldrich) and used as supplied. All samples were filtered before use using 0.2-mm hydrophilic polytetrafluoroethylene (PTFE) filters (Millipore) to remove dust. For all microscopy experiments, a sample thickness of 11.58 ± 0.19 μm was used, controlled by glass monodisperse particle standards (Whitehouse Scientific). Particles were sandwiched between borosilicate glass (VWR) and ruby mica discs, which were cleaned by rinsing in acetone, isopropyl alcohol, and distilled water, followed by drying in an oven at 150˚C for 30 mins. The sample temperature was controlled to ±0.1 K using a Linkam THMS600 microscopy stage. In the experiments, the samples were quenched and held at a selected temperature. [35,36]

Microscopy

Microscopy was carried out using an Olympus BX53 light microscope that features modular units for phase-contrast and fluorescence microscopy, and a custom unit allowing for simultaneous laser irradiation and microscopy. The laser used was a 785-nm diode laser (Thorlabs Ltd.) producing a maximum power incident on the sample of 200 mW with an elliptical mode with a mean beam radius (at half height) of 2.4 μm when using a 10× objective.

Phase-contrast microscopy converts small differences in optical path length into intensity, therefore it can be used as a measure of refractive index. Positive phase contrast has been used here and results intensity scaling with refractive index for objects on the micron scale. Nitrobenzene strongly quenches many fluorescent dyes, but the dye methylene blue is quenched relatively weakly. This produces contrast between the nitrobenzene rich and decane rich phases in fluorescence microscopy.

Data were captured using the ImageJ add-on Micro Manager and analysed primarily using ImageJ. IGOR was used to fit radial distribution profiles of droplets to Gaussian functions and graphing. The intensity of the LIPS effect (I_{LIPS}) shown in Figure 2 was calculated by determining the mean phase-contrast intensity within a droplet in ImageJ. The error bars shown in Figure 2(c) and (d) and Figure 3(g) and (h) are the ±1 standard deviation estimated through repeat measurements and are predominantly from laser power fluctuations.

Data availability

The data that support the findings of this study and were used to make figures 2 and 3 are available in Enlighten: Research Data Repository (University of Glasgow) with the identifier: http://dx.doi.org/10.5525/gla.researchdata.563.

References

1 Bučar, D.-K., Lancaster, R. W. & Bernstein, J. Disappearing Polymorphs Revisited. *Angew. Chem. Int. Ed.* **54**, 6972-6993 (2015).

2 Garetz, B., Aber, J., Goddard, N., Young, R. & Myerson, A. Nonphotochemical, polarization-dependent, laser-induced nucleation in supersaturated aqueous urea solutions. *Phys. Rev. Lett.* **77**, 3475-3476 (1996).

3 Garetz, B., Matic, J. & Myerson, A. Polarization switching of crystal structure in the nonphotochemical light-induced nucleation of supersaturated aqueous glycine solutions. *Phys. Rev. Lett.* **89**, 175501 (2002).

4 Ward, M. R., Mchugh, S. & Alexander, A. J. Non-photochemical laser-induced nucleation of supercooled glacial acetic acid. *Phys. Chem. Chem. Phys.* **14**, 90-93 (2012).

5 Iefuji, N. *et al*. Laser-induced nucleation in protein crystallization: Local increase in protein concentration induced by femtosecond laser irradiation. *J. Cryst. Growth* **318**, 741-744 (2011).

6 Usman, A., Uwada, T. & Masuhara, H. Optical Reorientation and Trapping of Nematic Liquid Crystals Leading to the Formation of Micrometer-Sized Domain. *J. Phys. Chem. C* **115**, 11906-11913 (2011).

7 Kosa, T. *et al*. Light-induced liquid crystallinity. *Nature* **485**, 347-349 (2012).

8 Knott, B. C., Larue, J. L., Wodtke, A. M., Doherty, M. F. & Peters, B. Communication: Bubbles, crystals, and laser-induced nucleation. *J. Chem. Phys.* **134**, 171102 (2011).

9 Knott, B. C., Doherty, M. F. & Peters, B. A simulation test of the optical Kerr mechanism for laser-induced nucleation. *J. Chem. Phys.* **134**, 154501 (2011).

10 Liu, Y., Van Den Berg, M. H. & Alexander, A. J. Supersaturation dependence of glycine polymorphism using laser-induced nucleation, sonocrystallization and nucleation by mechanical shock. *Phys. Chem. Chem. Phys.* **19**, 19386-19392 (2017).

11 Yuyama, K.-I., Rungsimanon, T., Sugiyama, T. & Masuhara, H. Selective Fabrication of α- and γ-Polymorphs of Glycine by Intense Polarized Continuous Wave Laser Beams. *Cryst. Growth. Des.* **12**, 2427-2434 (2012).

12 Tenwolde, P. & Frenkel, D. Enhancement of protein crystal nucleation by critical density fluctuations. *Science* **277**, 1975-1978 (1997).

13 Gebauer, D., Voelkel, A. & Coelfen, H. Stable Prenucleation Calcium Carbonate Clusters. *Science* **322**, 1819-1822 (2008).

14 Gebauer, D., Kellermeier, M., Gale, J. D., Bergström, L. & Cölfen, H. Pre-nucleation clusters as solute precursors in crystallisation. *Chem. Soc. Rev.* **43**, 2348-2371 (2014).
15 Radu, M. & Kremer, K. Enhanced Crystal Growth in Binary Lennard-Jones Mixtures. *Phys. Rev. Lett.* **118**, 055702-055706 (2017).
16 Wedekind, J. *et al*. Optimization of crystal nucleation close to a metastable fluid-fluid phase transition. *Sci. Rep.* **5**, 1-7 (2015).
17 Jones, R. a. L. *Soft Condensed Matter*. (Oxford University Press, 2002).
18 Bowman, R. W. & Padgett, M. J. Optical trapping and binding. *Rep. Prog. Phys.* **76**, 026401 (2013).
19 Yuyama, K.-I., George, J., Thomas, K. G., Sugiyama, T. & Masuhara, H. Two-Dimensional Growth Rate Control of l-Phenylalanine Crystal by Laser Trapping in Unsaturated Aqueous Solution. *Cryst. Growth. Des.* **16**, 953-960 (2016).
20 Méndez-Castro, P., Troncoso, J., Peleteiro, J. & Romaní, L. Heat capacity singularity of binary liquid mixtures at the liquid-liquid critical point. *Phys. Rev. E* **88**, 042107 (2013).
21 Gao, P., Yao, B., Harder, I., Lindlein, N. & Torcal-Milla, F. J. Phase-shifting Zernike phase contrast microscopy for quantitative phase measurement. *Opt. Lett.* **36**, 4305-4307 (2011).
22 Liu, Y., Ward, M. R. & Alexander, A. J. Polarization independence of laser-induced nucleation in supersaturated aqueous urea solutions. *Phys. Chem. Chem. Phys.* **19**, 3464-3467 (2017).
23 Duffus, C., Camp, P. J. & Alexander, A. J. Spatial Control of Crystal Nucleation in Agarose Gel. *J. Am. Chem. Soc.* **131**, 11676-11677 (2009).
24 Gutierrez, J. M. P., Hinkley, T., Taylor, J. W., Yanev, K. & Cronin, L. Evolution of oil droplets in a chemorobotic platform. *Nat. Commun.* **5**, 1-8 (2014).
25 Peterman, E. J. G., Gittes, F. & Schmidt, C. F. Laser-Induced Heating in Optical Traps. *Biophys. J.* **84**, 1308-1316 (2003).
26 Hofkens, J., Hotta, J., Sasaki, K., Masuhara, H. & Iwai, K. Molecular Assembling by the Radiation Pressure of a Focused Laser Beam: Poly(N-isopropylacrylamide) in Aqueous Solution. *Langmuir* **13**, 414-419 (1997).
27 Oana, H. *et al*. Spontaneous Formation of Giant Unilamellar Vesicles from Microdroplets of a Polyion Complex by Thermally Induced Phase Separation. *Angew. Chem. Int. Ed.* **48**, 4613-4616 (2009).
28 Kitamura, N., Yamada, M., Ishizaka, S. & Konno, K. Laser-Induced Liquid-to-Droplet Extraction of Chlorophenol: Photothermal Phase Separation of Aqueous Triethylamine Solutions. *Anal. Chem.* **77**, 6055-6061 (2005).
29 Bunkin, N. F., Lobeev, A. V., Lyakhov, G. A. & Svirko, Y. P. Local light-induced phase separation of binary liquid solutions. *Quantum Electron.* **26**, 60-64 (1996).
30 Osborne, M. A., Balasubramanian, S., Furey, W. S. & Klenerman, D. Optically Biased Diffusion of Single Molecules Studied by Confocal Fluorescence Microscopy. *J. Phys. Chem. B* **102**, 3160-3167 (1998).
31 Yuyama, K.-I., Sugiyama, T. & Masuhara, H. Laser Trapping and Crystallization Dynamics of l-Phenylalanine at Solution Surface. *J. Phys. Chem. Lett.* **4**, 2436-2440 (2013).
32 Wallace, A. F. *et al*. Microscopic evidence for liquid-liquid separation in supersaturated CaCO3 solutions. *Science* **341**, 885-889 (2013).
33 De Yoreo, J. J. *et al*. Crystallization by particle attachment in synthetic, biogenic, and geologic environments. *Science* **349**, aaa6760 (2015).
34 Masuhara, H., Sugiyama, T., Yuyama, K.-I. & Usman, A. Optical trapping assembling of clusters and nanoparticles in solution by CW and femtosecond lasers. *Opt. Rev.* **22**, 143-148 (2015).
35 Mosses, J., Syme, C. D. & Wynne, K. Order Parameter of the Liquid–Liquid Transition in a Molecular Liquid. *J. Phys. Chem. Lett.* **6**, 38-43 (2015).
36 Syme, C. D. *et al*. Frustration of crystallisation by a liquid–crystal phase. *Sci. Rep.* **7**, 42439 (2017).

Acknowledgments

We thank the Engineering and Physical Sciences Research Council (EPSRC) for support through grants EP/J004790/1, EP/J009733/1, and EP/N007417/1. We gratefully acknowledge discussions in 2010 with Colin Bain that planted the seed for this work.

Correspondence and requests for materials should be addressed to K.W.

Author Contributions

The experiments and data analysis were conducted by F.W., theory and simulations by K.W., both contributed to writing the paper. K.W. conceived the overall project. The authors declare no competing financial interests.

Figures

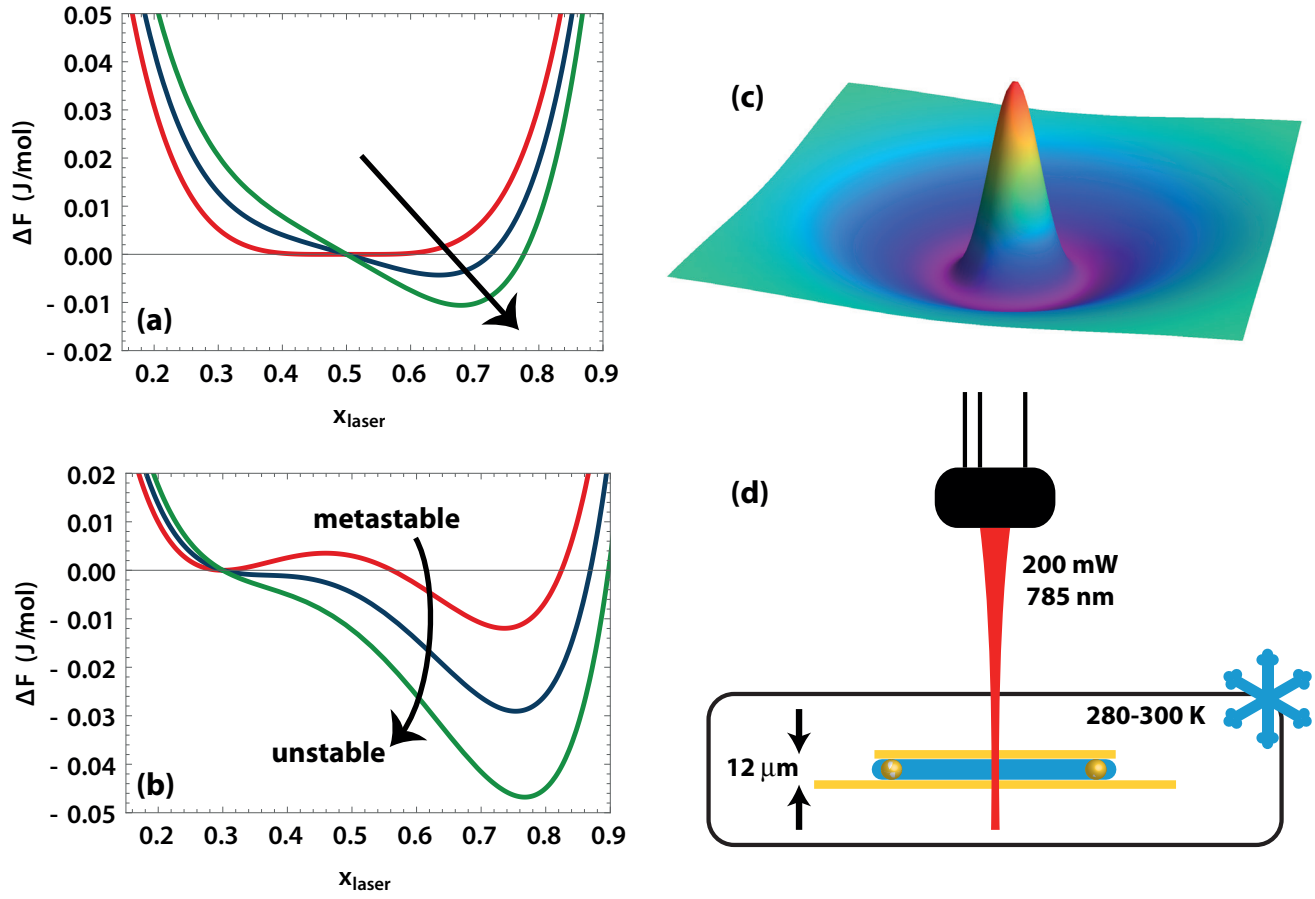

Figure 1. Summary of the laser-induced phase separation (LIPS) and laser-induced nucleation experiments. **(a)** A plot of the change in free energy ΔF in a nitrobenzene-decane mixture of mole fraction x_0 when the mole fraction is changed to x_{laser} in a small volume. Here the initial nitrobenzene mole fraction is $x_0 = 0.5$, the laser intensity is $I = 0$ (red), 100 (blue), and 200 (green) J/m^3. The other parameters are appropriate to a stable nitrobenzene-decane mixture (see supplementary section 1). As can be seen, when the laser power is increased, the minimum in the free-energy potential shifts to higher mole fraction causing phase separation through a diffusive concentration process. **(b)** As in (a) but with initial mole fraction $x_0 = 0.3$ and the other parameters appropriate to a metastable nitrobenzene-decane mixture. When the laser is off, a free-energy barrier prevents the system from phase separating spontaneously. However, with increasing laser power the barrier lowers and then disappears entirely, causing the system to transition from metastable to unstable, hence inducing nucleation of a new phase. **(c)** A three-dimensional plot of the position-dependent nitrobenzene mole fraction near the focus of a tweezing-laser. Laser-induced phase separation causes the nitrobenzene concentration to increase in the laser focus leaving behind a temporary depleted volume. **(d)** Cartoon of the experimental set-up consisting of a diode laser focussed in the sample, which is contained in a temperature-controlled cell (see Methods).

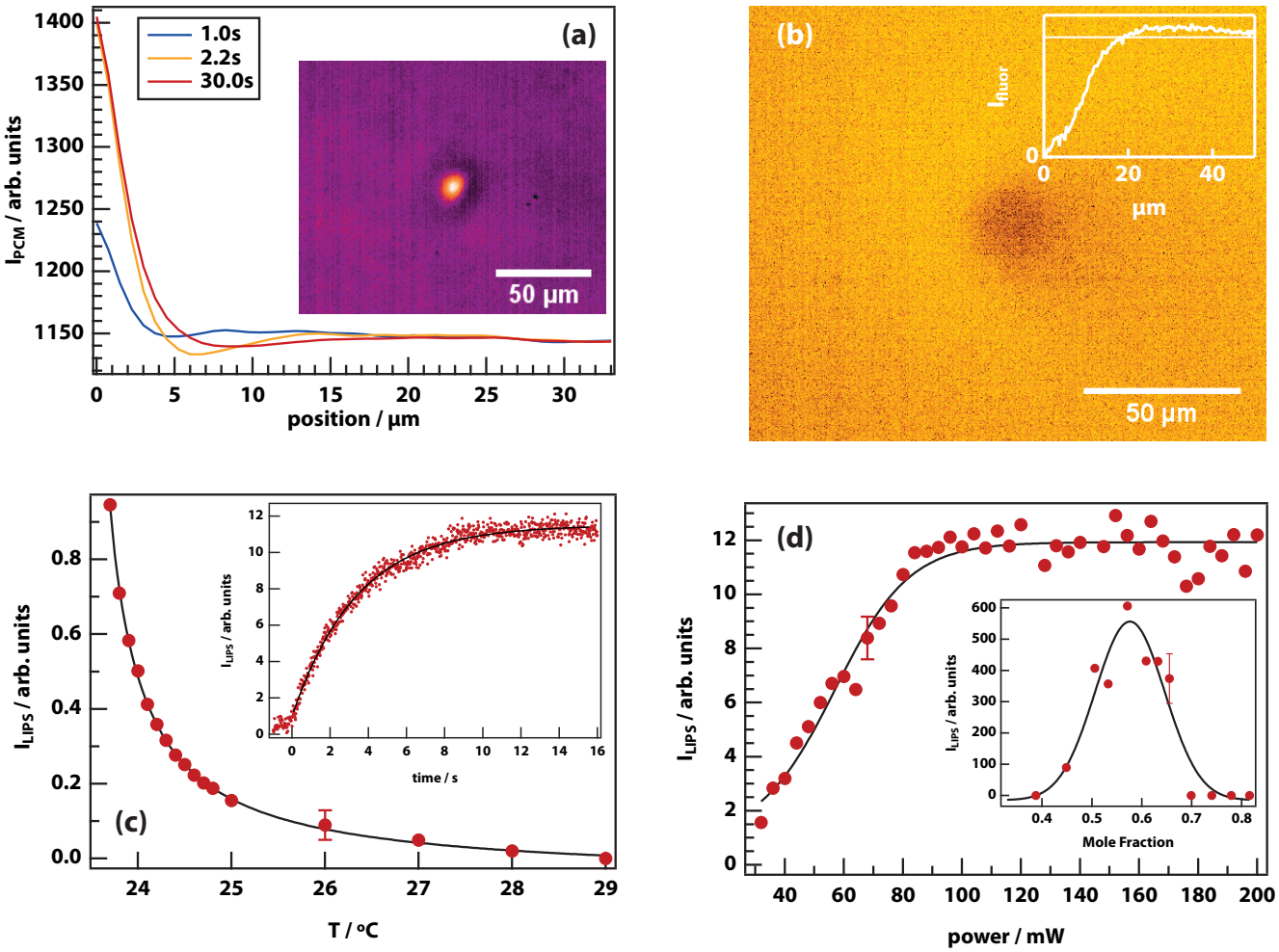

Figure 2. Experimental laser-induced phase separation (LIPS) through the tweezing effect. **(a)** Radial distributions of the LIPS droplet (mole fraction $x = 0.575$) measured using phase-contrast microscopy (PCM). They show a time-dependent enhancement of the nitrobenzene mole fraction in the focus of the tweezing laser and a depletion region at a radius of 4 to 10 µm. The vertical axis is the phase-contrast intensity at each point. Inset is a false-colour PCM image of the droplet. (**b)** False colour fluorescence image of a LIPS droplet (dark) showing fluorescence quenching demonstrating that it is nitrobenzene enriched. The inset shows the radial distribution of the fluorescence intensity. **(c)** Temperature dependence of the magnitude of the LIPS effect (defined as the mean phase-contrast intensity within a droplet) at $x = 0.575$ fit to an inverse power-law function demonstrating that the LIPS effect maximises on the liquid-liquid demixing binodal line. Inset is the magnitude of the LIPS effect as a function of delay time after the tweezing-laser switch on. The 3.4-s rise time is consistent with diffusion of nitrobenzene into the droplet. **(d)** The magnitude of the LIPS effect as a function of incident laser power. The inset shows the dependence on mole fraction (at an incident laser power of 70 mW) demonstrating enhancement of the LIPS effect near the liquid-liquid critical point.

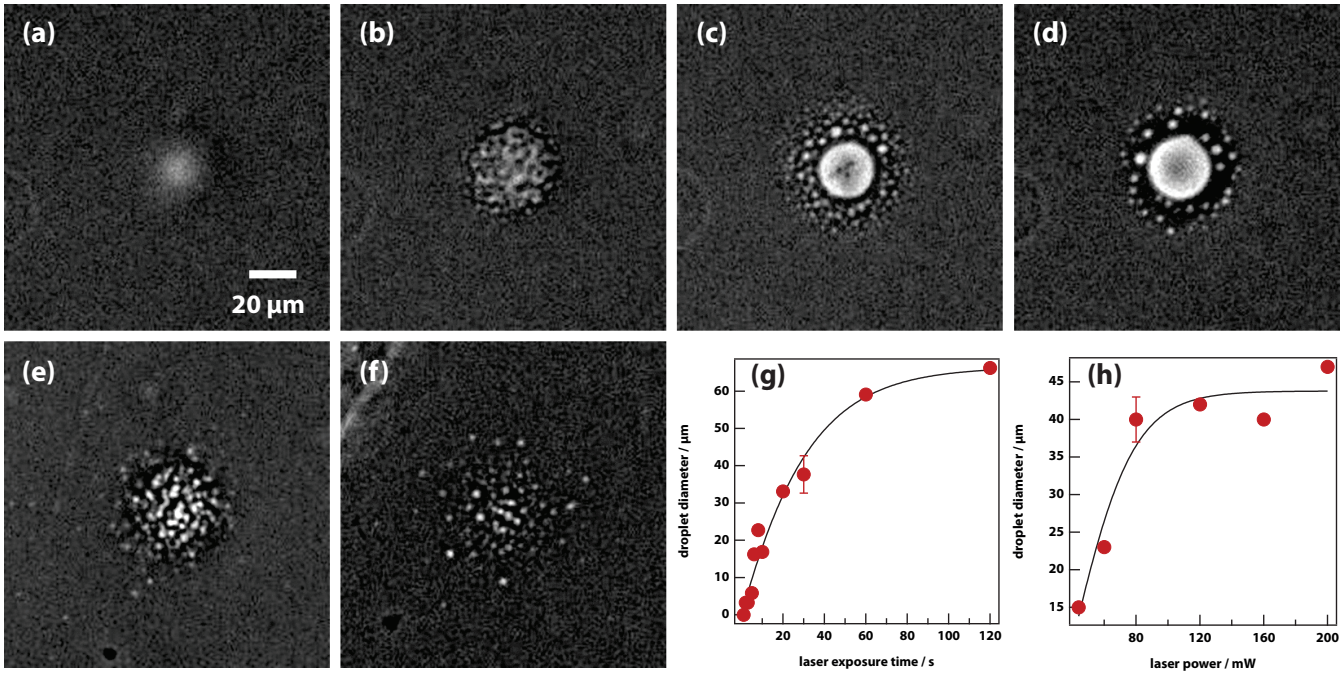

Figure 3. Laser-induced nucleation triggered via the LIPS effect. **(a)** In the mixed regime near a binodal, the LIPS effect combined with heating produces a droplet enriched in nitrobenzene surrounded by a depleted volume. (x = 0.632, T = 23.9°C, incident laser power 100 mW for 30 s, measured using phase-contrast microscopy) **(b)** Switching off the laser, puts the depleted volume in the metastable region, triggering nucleation after < 1 s. **(c)** Nucleation is followed by Ostwald ripening (frame at 4 s). **(d)** The ripened droplet remains stable for tens of minutes (frame at 14 s). **(e)** Further away from the critical point (here x = 0.657) the effect decreases (frame at 4 s). **(f)** As in (e) for x = 0.675 with a further diminished effect. **(g)** The diameter of the nucleated droplet (at x = 0.632) increases with laser exposure time and **(h)** also with laser power.

Control over phase separation and nucleation using a laser-tweezing potential - Supplementary information

Finlay Walton, Klaas Wynne*
School of Chemistry, WestCHEM, University of Glasgow, UK

Regular solution model of mixing

We will follow the modelling described by Jones,[1] and define a liquid mixture with mole fractions of molecule A and B given by x_0 and x_B, such that $x_B = 1\text{-}x_0$. Define an energy interaction term by

$$\chi = \frac{z}{2}\left(2\varepsilon_{AB} - \varepsilon_{AA} - \varepsilon_{BB}\right) \ . \tag{1}$$

The expression for the molar free energy is then

$$\begin{aligned} F_{mix}\left(x_0, T, \chi\right) &= RT\left(x_0 \ln x_0 + x_B \ln x_B\right) + \chi x_0 x_B \\ &= RT\left(x_0 \ln x_0 + \left[1 - x_0\right]\ln\left[1 - x_0\right]\right) + \chi x_0 \left(1 - x_0\right) \end{aligned} \tag{2}$$

Here $z\varepsilon_{AA}$ is approximately equal to the heat of vaporisation, which ranges from 0 (at the gas-liquid critical point) to ~40 kJ/mol. So, for poorly mixing liquids, χ is positive and on the order of a few kJ/mol.

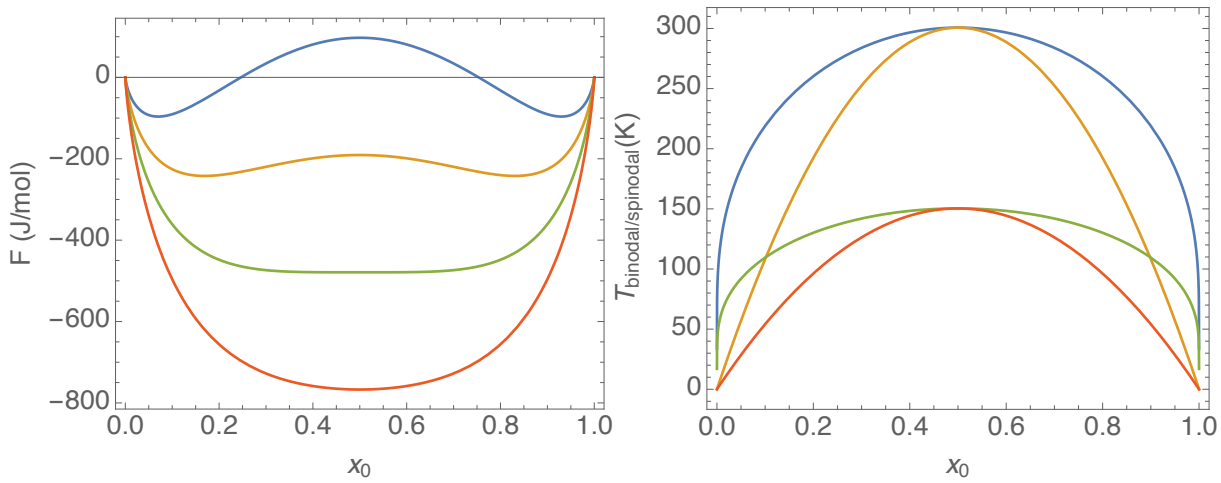

Figure 1. (left) Mixing free energy for χ = 5 kJ/mol and T = 200, 250, 300, and 350 K (top to bottom). (right) Binodal and spinodal for χ = 5 and 2.5 kJ/mol.

The coexistence curve is at $dF_{mix}/dx = 0$ and the spinodal at $d^2F_{mix}/dx^2 = 0$, which are easily solved for T as

$$T_{binodal} = \frac{\chi\left(1 - 2x_0\right)R^{-1}}{\ln\left(1 - x_0\right) - \ln\left(x_0\right)} \tag{3}$$

and

$$T_{spinodal} = 2x_0\chi\left(1 - x_0\right)R^{-1} \tag{4}$$

As can be seen in Figure 1, one obtains a reasonable representation of the decane-nitrobenzene binodal for χ = 5 kJ/mol.

Free-energy changes in a small volume

Suppose we have a volume V_0 of a mixture whose starting mole fraction of A is x_0. Now consider a tweezing laser with focal volume V_{laser}, which causes the mixture to change to mole fraction x_{laser} and the remaining volume V_{rest} with mole fraction x_{rest}.

$$V_0 = V_{laser} + V_{rest} \rightarrow V_{rest} = V_0 - V_{laser} \tag{5}$$

To conserve the total amount of A and B, we have

$$x_0 V_0 = x_{laser} V_{laser} + x_{rest} V_{rest} \rightarrow x_{rest} = \frac{x_0 V_0 - x_{laser} V_{laser}}{V_0 - V_{laser}} \tag{6}$$

The total energy of the phase-separated system is

$$F_{sep}\left(x_{laser}\right) = \frac{V_{laser}}{V_0} F_{mix}\left(x_{laser}\right) + \frac{V_{rest}}{V_0} F_{mix}\left(x_{rest}\right) \tag{7}$$

where V_{rest} and x_{rest} come from Eqs. (5) and (6). Figure 2 shows $\Delta F = F_{sep} - F\left(x_0\right)$.

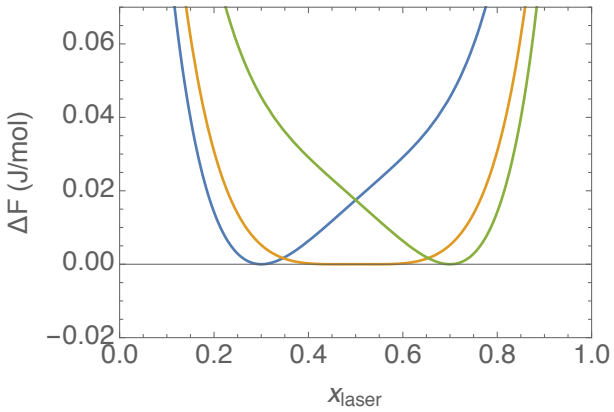

Figure 2. The change in free energy caused by changing the mole fraction in the laser volume for x_0 = 0.3, 0.5, and 0.7. T = 270 K.

Adding in the effect of a tweezing laser

The refractive index of a particular mixture is approximately given by

$$n\left(x\right) = x n_A + \left(1 - x\right) n_B \tag{8}$$

We will use the dipole approximation to calculate the stored electromagnetic energy. The stored electromagnetic energy is

$$U_{dip} = -PE = -\varepsilon_0 \chi E^2 = -\varepsilon_0 n^2 E^2, \left[U_{dip}\right] = \frac{J}{m^3} \ .$$

So, the total stored electromagnetic energy in the laser volume is

$$U_{laser} = -\varepsilon_0 n^2\left(x_{laser}\right) E^2 V_{laser} \ . \tag{9}$$

We can now plot the difference free energy including the effect of the laser

$$\Delta F_{sep,laser}\left(x_{laser}\right) = \frac{V_{laser}}{V_0} F_{mix}\left(x_{laser}\right) + \frac{V_{rest}}{V_0} F_{mix}\left(x_{rest}\right) - F_{mix}\left(x_0\right) - \left[n^2\left(x_{laser}\right) - n^2\left(x_0\right)\right] \varepsilon_0 E^2 V_{laser} \tag{10}$$

If the laser beam has a given energy flux (measured outside of the sample) of

$$U_{laser} = \varepsilon_0 E^2 Ac, \left[U_{laser}\right] = W \ , \tag{11}$$

where A is the area of the laser focus, then the laser intensity is

$$I = \varepsilon_0 E^2 = U_{laser} / Ac, \ \left[\varepsilon_0 E^2\right] = \frac{J}{m^3} \ , \tag{12}$$

For a typical ~200 mW laser (in the sample) focussed to a 2.4 μm radius spot, this gives ~40 kJ/m^3.

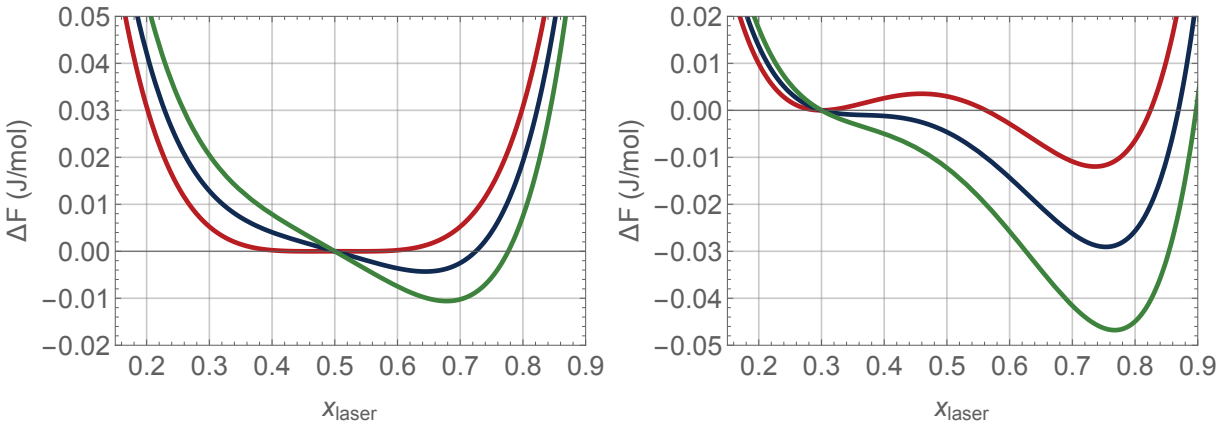

Figure 3. Additional details for Figure 1 in the main text. Plots of the change in free energy ΔF in a nitrobenzene-decane mixture of mole fraction x_0 of nitrobenzene when the mole fraction is changed to x_{laser} in a small volume. Here the initial nitrobenzene mole fraction is $x_0 = 0.5$ (left) and $x_0 = 0.3$ (right), the laser intensity is $I = 0$ (red), 100 (blue), and 200 (green) J/m^3, $\chi = 5$ kJ/mol, and $T = 300$ (left) and 280 (right) K. The refractive indices are set to $n_{decane} = 1.41$ and $n_{nitrobenzene} = 1.54$. The panel on the left corresponds to the regime in which the two liquids are mixed and close to the liquid-liquid critical point. In the panel on the right, the system is metastable when the laser is off and the free energy could be lowered by phase separation after crossing a free-energy barrier.

Change in refractive index calculation

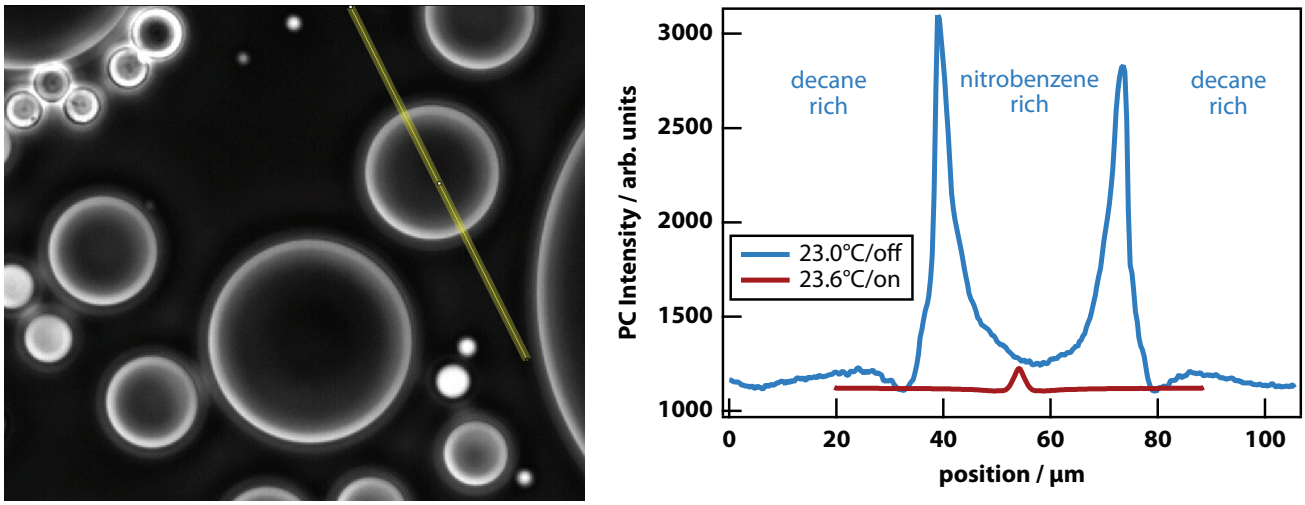

Figure 4. (**left**) Phase contrast image of a nitrobenzene–decane sample at the critical mole fraction (0.575) at a temperature (23.0°C) where phase separation has occurred. The line shows the cut through a nitrobenzene droplet. (**right**) Phase-contrast intensity along the cut line of a nitrobenzene–decane sample at the critical mole fraction at $T = 23.0$°C (phase separated) and $T = 23.6$°C (mixed) but in the presence of a LIPS-inducing laser. The curve at 23.0°C clearly shows saturation caused by the shade-off effect [2] inherent in phase-contrast microscopy of larger objects.

The composition of the LIPS-generated droplet can be calculated by estimating the changes in refractive index as measured on the edge of phase-separated droplets. From the cross sections of phase-contrast images shown in Figure 4, the droplet edges have amplitudes of 1820 and the LIPS droplet a central amplitude of 110. These values are proportional to the difference in refractive index Δn between them and the bulk. Using the lever rule in the phase diagram in Figure 5, the nitrobenzene-rich droplet and surrounding decane-rich region can be calculated to have mole fractions of 0.68 and 0.45 respectively. Under the reasonable assumption that the refractive index varies linearly with mole fraction, mole fractions of 0.68 and 0.45 correspond to refractive indices of 1.505 and 1.473 respectively. Therefore, $\Delta n = 0.032$ for the phase separated case, and the ratio 110/1820 can be used to calculate $\Delta n = 0.002$ for the LIPS droplet. Therefore $n = 1.493$ in the LIPS droplet compared to $n = 1.491$ in the bulk. We can now calculate the mole fraction of nitrobenzene in the LIPS droplet to be 0.589 compared to 0.575 in the bulk.

Nitrobenzene–decane phase diagram

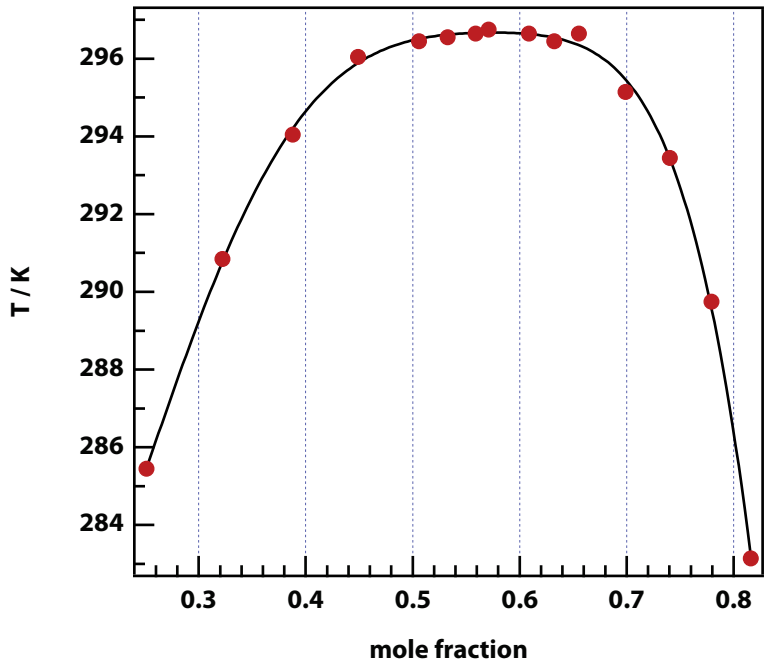

Figure 5. Nitrobenzene–decane phase diagram as measured in a 12-μm sample held between borosilicate glass slides. The red points indicate the highest temperature at which the demixed state is lower in energy than the mixed state. The black curve is for illustration only.

Sample heating calculation

Joule heating in the laser focus can be calculated using the model by Schmidt *et al.*,[3] where the rise in temperature in the focus is given by

$$\Delta T = \frac{\alpha P}{2\pi C_{th}}\left[\ln\left(\frac{2\pi R}{\lambda}\right) - 1\right], \qquad (13)$$

where α is the absorption coefficient (m^{-1}), P is the power (W), C_{th} is the thermal conductivity (J s^{-1} m^{-1} K^{-1}), R is the distance between the coverslips (m), and λ is the wavelength (m). Absorption coefficients were measured using UV-vis spectroscopy to be 0.698 m^{-1} for nitrobenzene and 0.684 m^{-1} for decane. Thermal conductivities at 25°C are 0.149 J s^{-1} m^{-1} K^{-1} for nitrobenzene and 0.1296 J s^{-1} m^{-1} K^{-1} for decane.[4] Hence, ΔT comes out as 0.50°C for nitrobenzene and 0.57°C for decane.

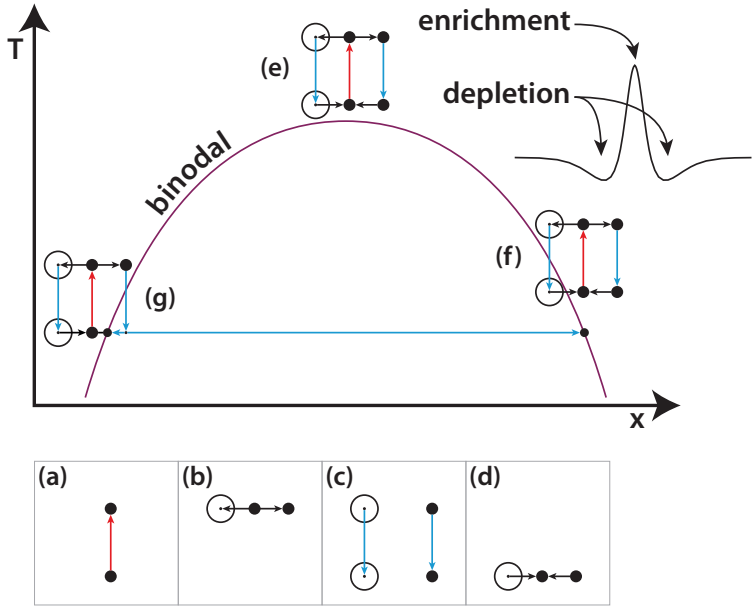

Figure 6. Schematic liquid-liquid phase diagram showing the combined effects of laser induced phase separation (LIPS) and heating. (a) When the tweezing laser is switched on, laser absorption will

quickly heat the laser volume and some of the surrounding area. **(b)** On a slower timescale, determined by mass diffusion, LIPS will cause the formation of a nitrobenzene enriched droplet surrounded by a depleted volume. **(c)** When the laser is switched off, both the enriched droplet and the depleted volume will quickly cool as thermal diffusion is 3 orders of magnitude faster than mass diffusion. **(d)** On a longer timescale equilibrium will be restored. **(e)** When such an experiment is carried near the critical point, nothing in particular happens as all points remain in the mixed region. **(f)** When the starting point is at high mole fraction and near the binodal, the depleted volume will drop into the meta- or un-stable region when the laser is switched off. **(g)** When the starting point is at low mole fraction and near the binodal, the enriched droplet will drop into the meta- or un-stable region when the laser is switched off. Phase separation will cause this droplet to further enrich while shrinking at the same time, rendering it invisible because of the lever rule.

References

1 Jones, R. a. L. *Soft Condensed Matter*. (Oxford University Press, 2002).

2 Gao, P., Yao, B., Harder, I., Lindlein, N. & Torcal-Milla, F. J. Phase-shifting Zernike phase contrast microscopy for quantitative phase measurement. *Opt. Lett.* **36**, 4305-4307 (2011).

3 Peterman, E. J. G., Gittes, F. & Schmidt, C. F. Laser-Induced Heating in Optical Traps. *Biophys. J.* **84**, 1308-1316 (2003).

4 *CRC Handbook of Chemistry and Physics*. Vol. 87 (CRC Taylor and Francis, 2006).